Inter-Chain Structure Factors of Flexible Polymers in Solutions: A Monte Carlo Investigation

V. Yamakov, A. Milchev, K. Binder

Inter-Chain Structure Factors of Flexible Polymers in Solutions: A Monte Carlo Investigation

V. Yamakov ([1]), A. Milchev ([1,2]) and K. Binder ([2,*])

([1]) Institute for Physical Chemistry, Bulgarian Academy of Sciences 1113 Sofia, Bulgaria
([2]) Institut für Physik, Johannes-Gutenberg-Universität-Mainz, Staudinger Weg 7, 55099 Mainz, Germany

(Received 22 November 1996, revised 21 March 1997, accepted 22 April 1997)

PACS.61.25.Hq – Macromolecular and polymer solutions; polymer melts; swelling
PACS.61.12.Ex – Neutron scattering techniques (including small-angle scattering)
PACS.61.20.Ja – Computer simulation of liquid structure

Abstract. — Off-lattice Monte Carlo simulations of both the single chain structure factor $h(q)$ and the inter-chain structure factor $H_D(q)$ of flexible polymers in solutions are presented over a wide range of both wavenumber q and concentration c from the dilute to the concentrated regime, for chain lengths up to $N = 256$. The single chain properties {gyration radius $\langle R_g^2\rangle$, $h(q)$} are in reasonable agreement with the expected theoretical behavior, showing a crossover from swollen chains $\{\langle R_g^2\rangle \propto N^{2\nu},\ h(q) \propto q^{-1/\nu}\}$ to Gaussian chains, and the data comply with a scaling description, with a correlation length $\xi \propto c^{-\nu/(3\nu-1)}$. However, the inter-chain structure factor $H_D(q)$ disagrees with the corresponding predictions, we find a behaviour $H_D(q) \propto q^{-3}$ only in an intermediate range but this is accidental: rather it is found that $H_D(q)$ smoothly bends over from its saturation value at small q to a behavior close to q^{-4} at $q \approx 1/\ell$, ℓ being the length of effective bonds. This failure is traced back to the condition that the law $H_D(q) \propto q^{-3}$ should only be observed for $\xi^{-1} \ll q \ll \ell^{-1}$, a condition reached neither in the simulation nor in experiments. We also compare our results for $H_D(q)$ with the random phase approximation and find strong deviations.

1. Introduction: A Review of the Problem of the Distinct Structure Factor $H_D(q)$

The structure of flexible polymers in a solution has been a topic of long-standing interest [1–6]. In a dilute solution under good solvent conditions, the single-chain structure factor $h(q)$, which describes the small angle neutron scattering intensity from (deuterated) chains under wave number q [3–5], reflects the size of the coil (as measured by its mean square gyration radius $\langle R_g^2\rangle$ at small q, N being the number of scattering monomers and c their concentration,

$$cNh(q) = cN\left(1 - \frac{1}{3}q^2\langle R_g^2\rangle + ..\right), \qquad q \ll \langle R_g^2\rangle^{-1/2} \tag{1}$$

while at larger q it contains information on the "fractal dimension" $d_f = 1/\nu$ of the chain,

$$h(q) \propto q^{-d_f}, \qquad \langle R_g^2\rangle^{-1/2} \ll q \ll \ell^{-1}, \tag{2}$$

(*) Author for correspondence (e-mail: binder@chaplin.physik.uni-mainz.de)

where ℓ is the typical distance between monomers.

In semidilute solutions, where the coils overlap, the chain structure is swollen as in the dilute case on length scales smaller than a screening length ξ only while for larger length scales the chains behave like ideal Gaussian random walks, *i.e.*

$$h(q) \propto q^{-2}, \quad \langle R_g^2 \rangle^{-1/2} \ll q \ll \xi^{-1}, \qquad \langle R_g^2 \rangle \propto \ell^2 \left(\frac{\xi}{\ell}\right)^{2-\ell/\nu} N, \tag{3}$$

while in the dilute case we have $\langle R_g^2 \rangle \propto \ell^2 N^{2\nu}$.

This picture of the single chain structure factor as sketched in equations (1-3) has been analyzed in detail by analytical theory [2,5], experiment [3,5] and simulations [7–9].

Of course, at finite concentration the total coherent scattering from a polymer solution (where all chains are thought to be labelled) contains also parts where *monomers belonging to different chains contribute.* Denoting the total volume of the system as V, we may define a total structure function $H_{\rm tot}(q)$ per monomer as

$$c^2 H_{\rm tot}(q) = \frac{1}{V} \sum_{a,b} \sum_{i,j=1}^{N} \langle \exp\left[i\mathbf{q} \cdot (\mathbf{r}_{ia} - \mathbf{r}_{jb})\right] \rangle, \tag{4}$$

where $\mathbf{r}_{ia}$ denotes the position of the i'th monomer of the a'th chain, and the sums run over all monomers of all chains. In contrast, the autocorrelation function $h(q)$ is defined by the analogous equation where only differences $\mathbf{r}_{ia} - \mathbf{r}_{ja}$ within the same chain contribute,

$$c\, N h(q) = \frac{1}{V} \sum_{a} \sum_{i,j=1}^{N} \langle \exp\left[i\mathbf{q} \cdot (\mathbf{r}_{ia} - \mathbf{r}_{ja})\right] \rangle. \tag{5}$$

In this work we focus on the part of the scattering in equation (4) due to interference of monomers from different chains [6]

$$c^2 H_{\rm D}(q) = \frac{1}{V} \sum_{a,b \neq a} \sum_{i,j}^{N} \langle \exp\left[i\mathbf{q} \cdot (\mathbf{r}_{ia} - \mathbf{r}_{jb})\right] \rangle, \tag{6}$$

which is related to the two scattering functions $H_{\rm tot}(q)$ and $h(q)$ trivially by

$$c^2 H_{\rm tot}(q) = cNh(q) + c^2 H_{\rm D}(\mathbf{q}). \tag{7}$$

It turns out that the behavior of $H_{\rm D}(q)$ is much less well-understood [1,6,10] than that of $H(q)$. The simplest approach to describe the collective scattering is due to the single-contact approximation (or random phase approximation, RPA), which yields [4–6]

$$c^2 H^0_{\rm tot}(q) = \frac{cNh(q)}{1 + bcNh(q)}, \tag{8}$$

where b is a constant representing two point interactions. While equation (8) is expected to be valid in systems with $d \geq 4$ spatial dimensions, where excluded volume interactions are relatively unimportant, it is clear that equation (8) is a rather poor approximation for $d = 3$ in dilute and semidilute solutions (at least for q comparable to the inverse screening length ξ^{-1}).

In contrast to the large q expansion that results from equation (8), $H^0_{\rm tot}(a) \propto q^{-2} -$ const. q^{-4}, renormalization group theory predicts a next-to leading q^3 power [6] (in $d = 3$ dimensions)

$$c^2 H^0_{\rm tot}(q) = a_1 \frac{c}{q^{1/\nu}} + a_2 \frac{c^2}{q^d} + a_3 \frac{c^{(d+\omega)/(d-1/\nu)}}{q^{2/\nu+\omega}} + \cdot \quad , \tag{9}$$

where ω is the correction to scaling exponent [11], and a_1, a_2, a_3 are constants. Equation (9) is believed to hold in the range $\xi^{-1} \ll q \ll \ell^{-1}$, in the semidilute regime ($\langle R_g^2 \rangle^{-1/2} \ll \xi^{-1}$). The first term on the right hand side of equation (9) is exactly the contribution of the autocorrelation function (Eq. (2)) and hence the distinct polymer structure function, $H_D(q)$ behaves as (*cf.* Eqs. (6, 7)), in d dimensions,

$$c^2 H_D(q) = a_2 \frac{c^2}{q^d} + a_3 \frac{c^{(d+\omega)/(d-1/\nu)}}{q^{2/\nu+\omega}} + \cdot \quad , \qquad \xi^{-1} \ll q \ll \ell^{-1} \tag{10}$$

While $\nu \approx 0.588$ is known rather precisely [11–16], the precise value of ω is still rather controversial: renormalization analyses yield [11–15] $\omega \approx 0.80 \pm 0.01$, while high-precision Monte Carlo estimates yield [16] $\omega \approx 0.95 \pm 0.04$. Hence the subleading term on the right hand side scales with wavevector like $q^{-4.20}$ or $q^{-4.35}$, and with concentration as $c^{2.92}$ or $c^{3.04}$ Since ξ scales as [4,5] $\xi/\ell \propto c^{-1/(d-1/\nu)}$, we can rewrite equation (10) also as

$$H_D(q) \propto q^{-d}[1 + \text{const}(q\xi)^{d-2/\nu-\omega} + \cdot \quad], \tag{11}$$

which reiterates the above conclusion that the simple behavior $H_D(q) \propto q^{-3}$ (in $d = 3$ dimensions) can only be observed for $q\xi \gg 1$.

Thus it is not surprising that an experimental study of this problem is very difficult: first of all both $H_{tot}(q)$ and $h(q)$ have to be measured separately and in absolute units, in order to allow the subtraction of both terms in equation (7) to isolate $H_D(q)$. Secondly, one has to be in the right regime, $\xi^{-1} \ll q \ll \ell^{-1}$

Experiments on this problem hence are scarce and not in mutual agreement with each other. Ullman *et al.* [10] accounted for their data in terms of the RPA expression (Eq. (8)) which implies $H_D(q) \propto q^{-4}$ rather than $H_D(q) \propto q^{-3}$, to leading order. Jannink *et al.* [6] find agreement with the leading term in equation (11), but their q-range on the log-log plot where they find deviations from the RPA and fit to $H_D(q) \propto q^{-3}$ ranges only from $\ln\{q[A^{0-1}]\} = \ln\xi^{-1} = -2.7$ to $\ln q_{max}[A^{0-1}] \approx -2.3$, *i.e.* only a small fraction (≈ 0.18) of a decade! To clearly identify an exponent, one wishes to have at least one decade of q for the fit on the log-log plot. In addition, the measured screening length ($\xi = (15 \pm 1)$ Å [6]) exceeds the step length of the effective units in polystyrene ($\ell \approx 6$ Å) only by a factor of 2.5, and hence the condition $\xi^{-1} \ll q \ll \ell^{-1}$ can never be satisfied in a strict sense. And there are even further experimental problems (subtraction of incoherent background, effects of polydispersity, *etc.* [6]).

Following a suggestion of Jannink [17], we attempt here to study $H_D(q)$ by Monte Carlo simulations, since the simulational approach should be ideal here:

(i) both $h(q)$ and $H_D(q)$ can be estimated directly and independently from the simulation configurations in a fairly straightforward way, and while the experimental q range is rather limited (the experiment [6] only had about a decade at its disposal, $9.4 \times 10^{-3}\ A^{0-1} \leq q \leq 10^{-1}$), this limitation is less present in the simulation (see Figs. 5, 6 below where the structure factors are presented for two decades of q rather than only one).

(ii) There is no incoherent background, no problem with a finite instrument resolution, no polydispersity (of course, we do not at all imply to criticize the experimental procedures applied in reference [6] to deal with these matters: we only imply that in our simulations we need not consider them at all).

(iii) Supplementary information (*e.g.* gyration radii, screening lengths, correlation functions in direct space, *etc.*) can be obtained from the same simulation.

However, as we shall see there is one major disadvantage of simulations that offsets to a large part the above advantages: this is the fact that for multichain system simulations at semi-dilute

solution conditions of only relatively short chains are possible. While for single chain studies it is now possible to generate and analyze self-avoiding walks, up to 80 000 steps [16], we have to restrict the present study to a chain length of $N \leq 256$ effective monomers: unlike also the experiment [6] for which N is of the order of 10^4, and the gyration radius ($\langle R_g^2 \rangle^{1/2} \approx 300$ Å [6]) is about 20 times larger than the screening length ξ, we are forced to work under conditions where $\langle R_g^2 \rangle^{1/2}$ is only a few times larger than ξ, and also ξ is only a few times larger than ℓ. Thus the simulation must have the problem that the observation of $H_D(q) \propto q^{-3}$ is hampered both at small q (a crossover controlled by $q\langle R_g^2 \rangle^{1/2}$ sets in if this variable is no longer very large) and at large q {where corrections of order $(q\xi)^{d-2/\nu-\omega} \approx (q\xi)^{-1.2}$ are expected (*cf.* Eq. (11)). Thus the conclusion of the simulations on the validity of equation (11) is also only preliminary. Nevertheless we describe here our results in detail, since to our knowledge the present work is the first simulation study of $H_D(q)$, and it yields interesting insight into the deviations from RPA.

One may ask whether it would be better to study rather a few very long chains in the dilute regime, rather than working mostly under semi-dilute conditions as we have done. We have not attempted to study very dilute cases, because then the "relaxation time" to equilibrate long range concentration fluctuations becomes prohibitively large, and only if these fluctuations are well-equilibrated is our $H_D(q)$ accurate enough. Also the statistical accuracy becomes worse in the dilute regime since the "events" contributing to $H_D(q)$ scale like c^2 while the simulation effort scales like c and thus for $c \to 0$ the "signal to noise" ratio becomes unfavorable, as in the experiment.

In Section 2, we briefly summarize the off-lattice bead-spring type model [8,18,19] on which the simulation is based, and discuss some pertinent details of computation and analysis. Section 3 summarizes our results on the single-chain properties, $\langle R_g^2 \rangle$ and $h(q)$, and estimates of ξ based on these quantities. Section 4 discusses the collective scattering, analyzing both $H_D(q)$ and the extent to which the RPA can describe these data, while Section 5 summarizes our conclusions.

2. The Off-Lattice Bead Spring Model, and Some Comments on the Monte Carlo Techniques Used for the Present Simulations

Each chain consists of N effective monomers, using $N = 32$, 64, 128, and 256. These beads are connected by springs which are given by the FENE potential (finitely extensible nonlinear elastic potential), where the bond length ℓ lies in the range $\ell_{min} \leq \ell \leq \ell_{max}$,

$$U_{FENE}(\ell) = -\frac{1}{2} K (\ell_{max} - \ell_0)^2 \ln \left[1 - (\ell - \ell_0)^2 / (\ell_{max} - \ell_0)^2 \right] . \tag{12}$$

The minimum of this potential occurs for $\ell = \ell_0$, $U_{FENE}(\ell_0) = 0$, and near ℓ_0 it is harmonic, with K being the spring constant. However, this potential diverges to infinity both when $\ell \to \ell_{min} = 2\ell_0 - \ell_{max}$ and when $\ell \to \ell_{max}$. We choose the parameters as $\ell_{min} = 0.4$, $\ell_0 = 0.7$, $\ell_{max} = 1$ (this is our unit of length), and $K/k_BT = 40$. The chains are treated as being fully flexible, and thus neither bond angle potentials nor torsional potentials are included: every effective bond is thought to represent $n \approx 3 - 6$ successive chemical bonds along the backbone of the chain, *i.e.* ℓ_0 is of the order of the persistence length.

As nonbonded interaction we use the Morse potential

$$U_M(r)/\varepsilon_M = \exp[-2\alpha(r - r_{min})] - 2\exp[-\alpha(r - r_{min})] \tag{13}$$

with parameters $r_{min} = 0.8$, $\alpha = 24$ and $\varepsilon_M = 1$ (we choose units such that Boltzmann's constant $k_B \equiv 1$). For this model it is known that the Theta temperature occurs at $\theta = 0.62$

[19], and working at $T = 1$ we hence are well within the good solvent regime. The particular advantage of this Morse potential is that it is very short-ranged and hence a link-cell algorithm with a cell size of unity can be used. We simulate then systems of size $L \times L \times L$ with periodic boundary conditions, choosing typically $L = 32$ (only for the dilute system with $c = 0.125$ and $c = 0.25$ linear dimension $L = 64$ was used for the sake of better statistics). Monomer concentrations studied were $c = 0.125$, 0.25, 0.50, 0.75, 1.0, 1.5 and 2.0 (note that with our choice of units of length the range $1.5 \leq c \leq 2.0$ corresponds to dense polymer melts [8,18,19]). Thus our systems are large enough so we have at least $\mathcal{N} = 128$ chains in the system, to avoid trivial finite size effects [9]. Note that due to the periodic boundary conditions, $H_{\mathrm{D}}(q)$ can be calculated only for discrete $\mathbf{q}$ vectors given by $\mathbf{q} = (2\pi/L)\,(\nu_x, \nu_y, \nu_z)$ where the ν_a are integers in the range from $1 \leq \nu_a \leq L$. However, this discreteness of reciprocal space is a limitation for very small q only, a region that is not of interest here. In the following, we measure q in units of $1/L$.

The structure factors $h(q)$, $H_{\mathrm{D}}(q)$ in our system are calculated by using the corresponding radial distribution functions. Performing a spherical average over the direction of $\mathbf{q}$, equations (5), (6) can be written

$$cNh(q) = \frac{1}{L^3}\left[\mathcal{N}N + 2\sum_{\alpha=1}^{\mathcal{N}}\sum_{n=1}^{N-1}\sum_{m>n}^{N}\sin(q|\mathbf{r}_{n\alpha} - \mathbf{r}_{m\alpha}|)/(q|\mathbf{r}_{n\alpha} - \mathbf{r}_{m\alpha}|)\right], \tag{14}$$

$$c^2 H_{\mathrm{D}}(q) = \frac{2}{L^3}\sum_{\alpha=1}^{\mathcal{N}}\sum_{\beta=1}^{\mathcal{N}}{}'\sum_{n=1}^{N-1}\sum_{m>n}^{N}\sin(q|\mathbf{r}_{n\alpha} - \mathbf{r}_{m\beta}|)/(q|\mathbf{r}_{n\alpha} - \mathbf{r}_{m\beta}|), \tag{15}$$

the prime on the sum over β in equation (15) means that only monomers of different chains contribute ($\alpha \neq \beta$).

We now replace the summations over monomer indices in equations (14), (15) by an integration over $r = |\mathbf{r}_{n\alpha} - \mathbf{r}_{m\alpha}|$ or $r = |\mathbf{r}_{n\alpha} - \mathbf{r}_{m\beta}|$, respectively; because of the periodic boundary conditions it does not make any sense to consider distances $r > L/2$, and thus these integrations are cut off at the half linear dimension of the box. Noting that $c = \mathcal{N}N/L^3$, we have

$$cNh(q) = c\left[1 + \int_0^{L/2} 4\pi r^2 c G_{\mathrm{s}}(r)\frac{\sin qr}{qr}\mathrm{d}r\right], \tag{16}$$

$G_{\mathrm{s}}(r)$ being the radial density distribution function of monomers belonging to the same chain. Similarly

$$c^2 H_{\mathrm{D}}(q) = c\int_0^{L/2} 4\pi r^2 c G_{\mathrm{D}}(r)\frac{\sin qr}{qr}\mathrm{d}r, \tag{17}$$

where $G_{\mathrm{D}}(r)$ is the radial density distribution function of monomers belonging to distinct chains. In the thermodynamic limit, equation (17) produces a delta function at $q = 0$, and this fact creates difficulties with the numerical integration of equation (17) for finite L. Therefore it is necessary to split the integral in two parts using $r^2 G_{\mathrm{D}}(r) = r^2[G_{\mathrm{D}}(r) - 1] + r^2$, noting that the integral $\int r^2 \sin qr/(qr)\mathrm{d}r$ yields the delta function and can be omitted. Thus we can compute $S_{\mathrm{D}}(q)$ as

$$H_{\mathrm{D}}(q) = 4\pi\int_0^{L/2} r^2[G_{\mathrm{D}}(r) - 1]\frac{\sin qr}{qr}\mathrm{d}r. \tag{18}$$

The total radial distribution function $G(r) = G_{\mathrm{s}}(r) + G_{\mathrm{D}}(r)$ can also be used to estimate the correlation length, from the standard formula

$$\xi^2 = \frac{1}{6}\int_0^{\infty} r^2[G(r) - 1]r^2\mathrm{d}r \Big/ \int_0^{\infty}[G(r) - 1]r^2\mathrm{d}r. \tag{19}$$

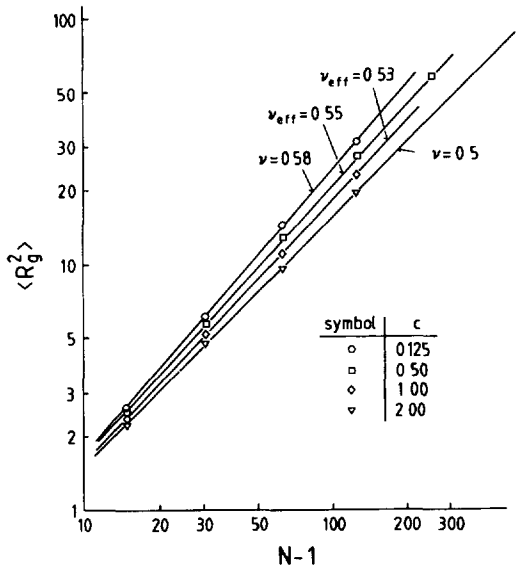

Fig. 1. — log-log plot of the mean-square gyration radius of $\langle R_g^2 \rangle$ *vs.* the number of bonds $N-1$ for four concentrations c as indicated. Straight lines indicate power laws $\langle R_g^2 \rangle \propto N^{2\nu_{eff}}$ with effective exponents as quoted in the figure. Statistical errors of $\langle R_g^2 \rangle$ are smaller than the size of the symbols.

This formula is difficult to use in practice in our case, since statistical errors at large r cause rather erratic contributions to the integral in the numerator. Thus we have used the following procedure, where we first split off the intra-chain part and integrate $G_D(r)$ only up to a cutoff L_0, while for $r > L_0$ we integrate an exponential fit $A_0 \exp(-r/\xi_0)$ performed in the region $2 \leq r \leq L_0$, where the statistical errors of $G_D(r) - 1$ are still not too large:

$$\xi^2 = \frac{1}{6} \frac{\langle R_g^2 \rangle + 4\pi \int_0^{L_0} r^2 [G_D(r) - 1] r^2 dr + 4\pi A_0 \int_{L_0}^{\infty} r^4 \exp(-r/\xi_0) dr}{(N-1) + 4\pi \int_0^{L_0} [G_D(r) - 1] r^2 dr + 4\pi A_0 \int_{L_0}^{\infty} r^2 \exp(-r/\xi_0) dr}. \tag{20}$$

Finally we note that the Monte Carlo algorithm used is the same as in previous work [8,18,19], *i.e.* monomers are chosen at random and one attempts a move to randomly chosen new coordinates $\mathbf{r}'$ in a cube of linear size $\Delta = 1$ centered around the old coordinate. From equations (12, 13) one computes the change in potential energy ΔU and the transition probability $W = \exp(-\Delta U/T)$, applying the standard Metropolis criterion [9]. For dilute systems, this algorithm has an acceptance rate of about 15%, which however decreases to the one percent range for dense melts.

3. Single Chain Properties

As pointed out in Section 1, it is crucial to examine $H_D(q)$ in the right regime of wavevectors and concentrations. To find this regime, we have to analyze single-chain properties first.

Figure 1 shows some of our data for $\langle R_g^2 \rangle$ *vs.* $N-1$ on a log-log plot. It is seen that in the dilute case ($c = 0.125$) the data are compatible with a power law $\langle R_g^2 \rangle \propto N^{2\nu}$ with $\nu \approx 0.58$,

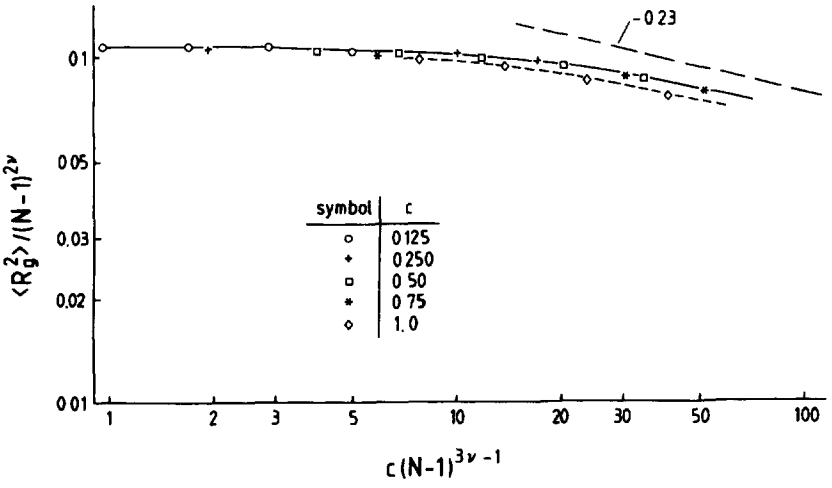

Fig. 2. — log-log plot of $\langle R_g^2 \rangle / (N-1)^{2\nu}$ *vs.* $c(N-1)^{3\nu-1}$, for concentrations c in the range $0.125 \leq c \leq 1$, as indicated, using data from $N = 16$ to $N = 256$ (the latter size is available only for $0.25 \leq c \leq 0.75$). Full curve is a tentative estimate of the scaling function, asymptotic slope of the scaling function, $-(2\nu-1)/(3\nu-1) \approx -0.23$, is indicated by the dash-dotted line. Note that data for $c = 1.0$ deviate from the crossover scaling function already systematically (diamonds connected by broken curve).

close to the theoretically expected value. With increasing concentration the crossover towards Gaussian behavior shows up in a gradual reduction of the "effective exponent" ν_{eff} which has reached the Gaussian value $\nu = 0.5$ for the dense melts. Note that the data for $\langle R_g^2 \rangle$ are not obtained from a "Zimm plot" but are directly calculated from the configurations of the polymer chains invoking the definition $\langle R_g^2 \rangle = \frac{1}{N} \sum_{i=1}^{N} \langle (\mathbf{r}_i - \mathbf{R}_{\text{cm}})^2 \rangle$, $\mathbf{r}_i$ being the coordinate of the i'th monomer of a chain and $\mathbf{R}_{\text{cm}}$ its centre of mass coordinate. Since for the present range of N in Figure 1 there are still some effects of corrections to scaling to the asymptotic power laws to be expected [16], one should not take the deviation of our value $\nu \approx 0.58$ from the theoretically expected one [5,11,16] $\nu \approx 0.59$ seriously.

Of course, a more sensible presentation of this crossover is possible by carrying out a scaling analysis, *i.e.* we plot $\langle R_g^2 \rangle / (N-1)^{2\nu}$ *vs.* $c(N-1)^{3\nu-1}$ using the theoretical value of $\nu = 0.588$ [5,11] (see Fig. 2). It is seen that the Monte Carlo results for $0.125 \leq c \leq 0.75$ are reasonably well consistent with the crossover scaling description, while data for $c = 1.0$ (*i.e.* half the monomer density of a dense melt) fall systematically below the scaling function (data for $c = 1.5$ and $c = 2$ would fall even further below and clearly are outside the crossover scaling regime).

From Figure 2 we can estimate the overlap concentration c^*, where a significant decrease of the chain linear dimensions sets in, as $c^*(N-1)^{3\nu-1} = 20$. This yields $c^*(N = 128) \approx 0.494$ and $c^*(N = 256) \approx 0.290$. Thus we see that chain lengths $N \geq 128$ and concentrations $c \geq 0.5$ are required, in order to work in the semidilute regime. On the other hand, $c < 1$ is needed since for $c \geq 1$ the solution is already too concentrated, so that clearly we cannot reach semidilute concentrations for which c/c^* is large (unlike the experiment where $c/c^* = 17$ is quoted [6]): this would require to simulate much longer chains, which is impossible for the present model (and simulation technique).

Of course, there is some arbitrariness in this estimation of the prefactor in the relation for the overlap concentration, $c^* \propto (N-1)^{-(3\nu-1)}$ An alternative estimate of c^* is based on the approach where one uses the spherical volume associated with the gyration radius in the dilute limit, $\langle R_g^2 \rangle_{c=0}^{1/2}$, assuming that at $c = c^*$ the overall concentration is equal to the density inside this spherical volume, $\rho = N/V = 3N/(4\pi \langle R_g^2 \rangle^{3/2})$. Since (Fig. 2) $\langle R_g^2 \rangle \approx 0.11\ (N-1)^{2\nu}$, we obtain $c^* \approx 6.54\ (N-1)^{-(3\nu-1)}$, *i.e.* a three times smaller prefactor. Using the latter estimate of c^* and the concentration dependence of the screening length [4,5]

$$\xi(c) = \xi_0 c^{-\nu/(3\nu-1)} \approx \xi_0 c^{-0.77} \tag{21}$$

to equate $\xi(c^*) = \langle R_g^2 \rangle^{1/2}$, we obtain $\xi_0 \approx 1.38$, *i.e.* $\xi(c = 0.25) \approx 4.01$, $\xi(c = 0.5) \approx 2.35$ and $\xi(c = 0.75) \approx 1.72$. Since in our (fully flexible) model the effective bond length ℓ is roughly equal to $\ell_0 = 0.7$, we see that the simulation has the same problem as the experiment, namely the range from ℓ to ξ is rather limited (and this fact makes the test of Eq. (11) difficult, see Eq. (10)).

Next we turn to the single chain structure factor $h(q)$ (Fig. 3). It is seen that in both the dilute case (Fig. 3a) and in the melt case (Fig. 3b) the theoretically predicted behavior (Eqs. (2, 3)) is readily verified; in the semidilute case (Fig. 3c) the crossover shows up in terms of an intermediate value $\nu_{\text{eff}} \approx 0.55$ for the effective exponent in a power law $h(q) \propto q^{-1/\nu_{\text{eff}}}$, compatible with the N-dependence of $\langle R_g^2 \rangle$ (Fig. 1). It is gratifying that the region where the power laws are observed is not as severely restricted as written in equations (2, 3): it is enough that q exceeds the lower limit by about a factor of 1.5 to reach the region where the power law holds, and on the upper end q_2 (given by the inverse bond length ℓ_0 both in the dilute case and in the melt) the condition $q < q_2$ is not serious at all, *i.e.* one even may exceed q_2 by a factor of 1.5. On the other hand, in the semidilute case the inverse screening length ξ^{-1} (related to q_ξ, Fig. 3c) and $\langle R_g^2 \rangle^{-1/2}$ are too close together, and at $q \lesssim q_\xi$ the saturation of $h(q)$ according to equation (1) is already a little bit felt: thus we are unable to verify the classical behavior $h(q) \propto q^{-2}$ in the semidilute regime (simply because our available chain lengths are still far too short). This point is examined further in Figure 3d, where a plot of $q^2 h(q)$ is given for $c \geq 0.5$. It is seen that for $c \geq 1$ there is an essentially horizontal part in the q-range from $q \approx 0.9 \times 10^{-1}$ to $q \approx 4 \times 10^{-1}$, while for $c = 0.5$ this horizontal part is shorter, ranging only from $q \approx 0.9 \times 10^{-1}$ to $q \approx 1.5 \times 10^{-1}$, because now q_ξ lies in this range. But the available q-range clearly is too small to identify both regions with $\nu = 0.5$ and $\nu = 0.59$ here. Therefore, the data for $h(q)$ are not well-suited for extracting an estimate for $\xi(c)$, unlike a related study of the bond fluctuation model [7].

Finally we turn to our attempts to directly extract the concentration dependence from the pair correlation function Figure 4, as given in equations (19, 20). The numbers obtained in this way are $\xi(c = 0.25) \approx 1.23$, $\xi(c = 0.5) \approx 1.12$, and $\xi(c = 0.75) \approx 1.05$. These numbers are significantly smaller than the above estimates quoted after equation (21). On the other hand, there is better agreement with the estimates $\xi_0(c = 0.25) \approx 2.5$, $\xi_0(c = 0.50) \approx 2.2$, $\xi_0(c = 0.75) \approx 2.1$. However, it was found that both estimates for ξ_0 increase somewhat when one repeats this analysis for $N = 256$ instead for $N = 128$. Thus he accuracy of this direct estimation of ξ seems to be rather uncertain.

4. Simulation Results for the Inter-Chain Structure Function $H_D(q)$

Typical data for the various structure factors are given in Figure 5. Note that for large q the total structure factor and the intrachain structure factor coincide, because there the correction due to inter-chain contributions is negligible. For $c \to 0$, equation (7) implies that $\frac{c}{N} H_{\text{tot}}(q)$

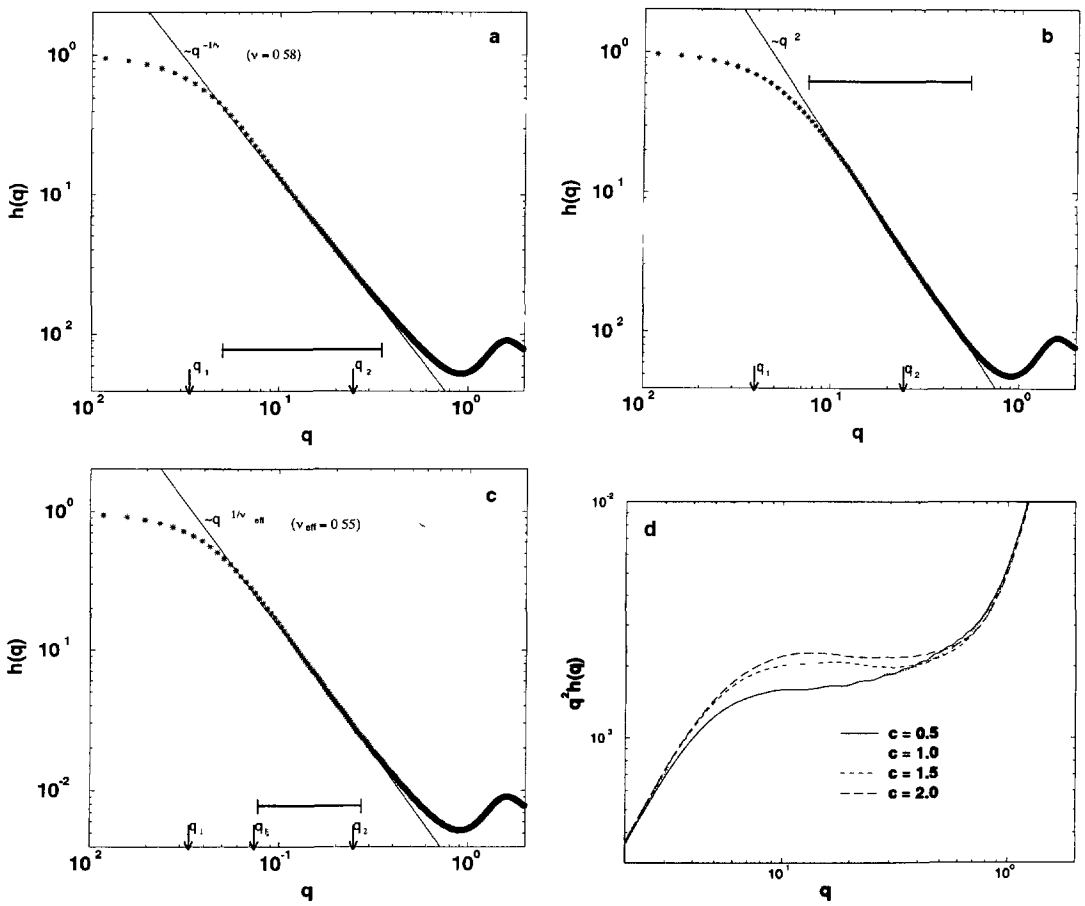

Fig. 3. — log-log plot of the normalized single chain structure factor $h(q)$ *vs.* q (in units of $1/L$ rather than $2\pi/L$), a) for the case $c = 0.125$, $L = 64$, $N = 128$ and b) the case $c = 2.0$, $L = 32$, $N = 128$. Arrows show $q_1 = (2\pi\langle R_g^2\rangle^{1/2})^{-1}$ and $q_2 = (2\pi\ell_0)^{-1}$, and the horizontal bar indicates the range over which equation (2) or equation (3) is fitted to the data. c) shows the case $c = 0.5$, $L = 32$, $N = 128$ and includes also the wavenumber $q_\xi = (2\pi\xi)^{-1}$, using the estimate $\xi = 2.35$ quoted in the text. d) log-log plot of $q^2h(q)$ *vs.* q for four concentrations, as indicated in the figure.

(the quantity that is actually plotted) coincides with $h(q)$, the single chain structure factor. We see that even for the dilute case, $c = 0.125$, where for $N = 128$ $\langle R_g^2\rangle^{-1/2}$ and ξ are comparable (Eq. (21) would predict $\xi = 6.84$, while $\langle R_g^2\rangle^{-1/2} = 5.61$) the deviations of $\frac{c}{N}H_{\rm tot}(q)$ from $h(q)$ for small q are already quite large. The larger the concentration the more pronounced does this deviation become. A similar concentration dependence of $H_{\rm tot}(q)$ is also well-known experimentally (*e.g.* Zimm [20]).

In order to work out the RPA, we note from equation (8) that the "constant" bcN can be expressed as follows

$$bcN = \left[\frac{c}{N}H^0_{\rm tot}(q)\right]^{-1} - h^{-1}(q). \tag{22}$$

In reality, equation (22) will not be exact, and the left hand side of this equation will be

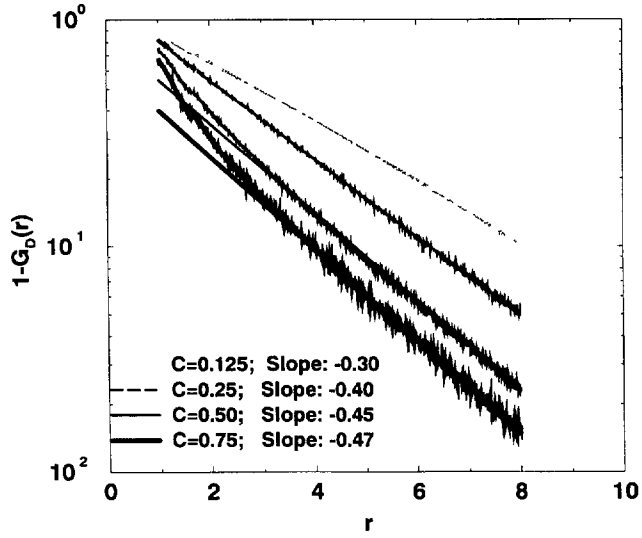

Fig. 4. — Semi-log plot of $1 - G_D(r)$ *vs.* r, for $N = 128$ and four concentrations as indicated. Straight lines show fits $A_0 \exp(-r/\xi_0)$, $-A_0$ being the intercept at the ordinate, and $-1/\xi_0$ is the slope quoted in the figure, choosing $L_0 = 8$ here.

q-dependent. To avoid this problem, we define bcN as the limit of equation (22) resulting for $q \to 0$ from our simulation data. The resulting constant is then used for the RPA expression for $H_D(q)$, namely

$$\frac{c}{N}\, {}^0H_D(q) \equiv -\frac{bcNh^2(q)}{1 + bcNh(q)}, \tag{23}$$

that has been computed from the single-chain structure factor $h(q)$ as observed in the simulation, and is included in Figure 5. Due to this procedure, there is trivially an agreement between the actual inter-chain structure factor $(c/N)H_D(q)$ and the RPA result (Eq. (23)) for $q \to 0$, but apart from this constant there are no other adjustable parameters whatsoever involved in this comparison.

While in the dilute case ($c = 0.125$) the RPA predicts a decay of the inter-chain structure factor which is too slow for large q, the behavior is opposite for the semidilute case: for $q > q_2 = (2\pi\ell_0)^{-1}$ the actual inter-chain structure factor $H_D(q)$ is larger than the RPA prediction: this deviation goes in the same direction as was observed in the experiment of Jannink *et al.* [6]. Note that the behavior for $c = 0.5$ is similar, and also the behavior of the longer chain length ($N = 256$) is similar.

Should we attribute these deviations form RPA then to the prediction $H_D(q) \propto q^{-d}$ (Eq. (11)), as done in reference [6]? To analyze this problem, Figure 6 gives a slightly enlarged view of $H_D(q)$ alone, for $N = 256$ and the three concentrations $c = 0.25$, 0.50, and 0.75, which one might consider as candidates for this analysis. To emphasize that we are working in a useful range of wavenumbers, the estimates for $q_1 = (2\pi\langle R_g^2\rangle)^{-1}$, $q_\xi = (2\pi\xi)^{-1}$ and $q_2 = (2\pi\ell_0)^{-1}$ are shown by arrows.

While the single chain structure factor (Fig. 3) did show a very good power law around q_2, this is clearly not the case here. Slopes at $q = 10^{-1}$ and at q_2 are emphasized by straight lines, and even larger effective exponent close to minus four results for $q > q_2$, but it is clear that these numbers do not have any particular significance, since they strongly depend both on c

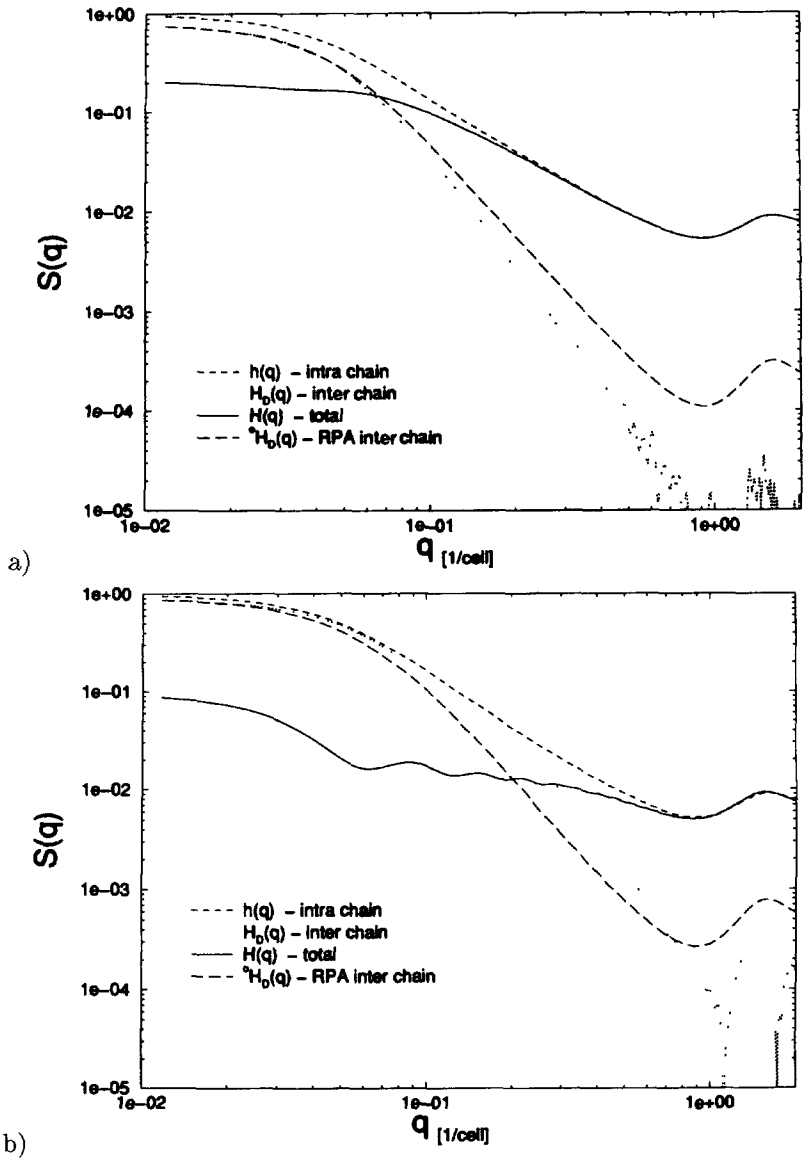

Fig. 5. — log-log plot of various structure factors {denoted symbolically as $S(q)$} *vs.* q (in units of $1/L$), for $N = 128$ and two concentrations: $c = 0.125$ (a) and $c = 0.75$ (b). Both the intra-chain structure factor $h(q)$, the inter-chain structure factor $H_D(q)$, the total structure factor $H(q)$ and the RPA-inter-chain structure factor ${}^0H_D(q)$ are included. Note that a factor c/N has been absorbed in the normalization of the total and inter-chain structure factors.

and on q. Again slightly different numbers result for the smaller chain length, $N = 128$, but since there q_ξ is somewhat closer to q_1, some residual influence of the finite gyration radius is to be expected. In Figure 6d we compare $H_D(q)$ for $N = 64$, for $N = 128$ and $N = 256$ and $c = 0.5$ to show that in the relevant q range a N-independent structure factor is indeed obtained, as it should be in the semidilute concentration regime: hence one cannot discard our

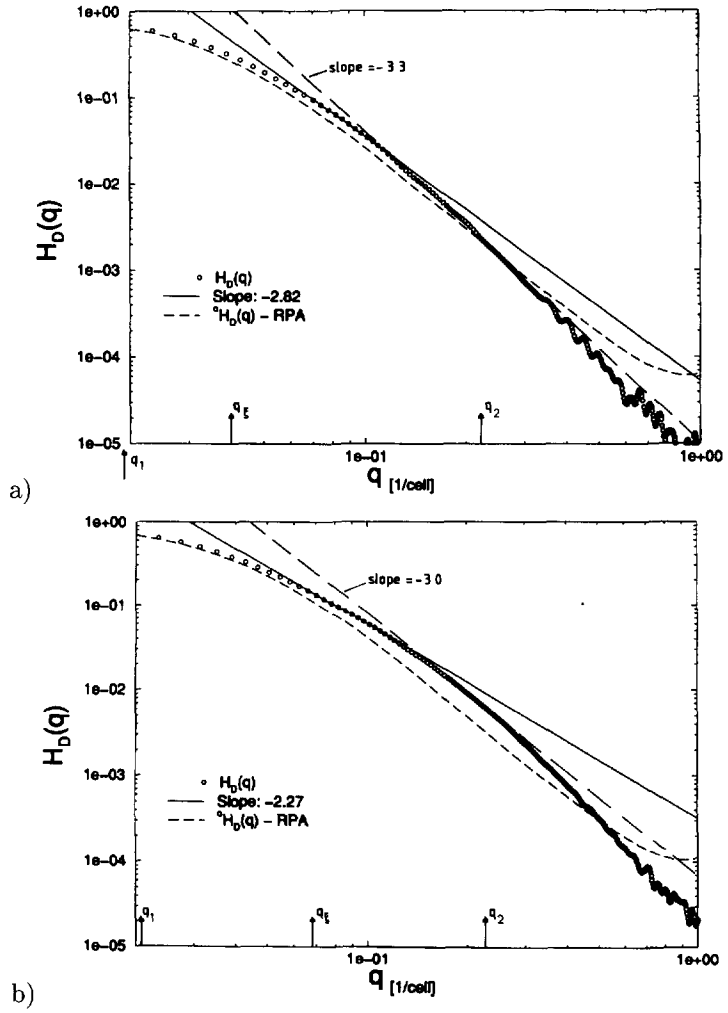

Fig. 6. — log-log plot of inter-chain structure factor $H_D(q)$ *vs.* q, for $N = 256$ and four concentrations: $c = 0.25$ (a), $c = 0.50$ (b), $c = 0.75$ (c) and $c = 2.0$ (e). Dots are Monte Carlo data, while broken curves show the RPA result. Full and dash-dotted straight lines indicate possible power law fits at $q = 10^{-1}$ and $q = q_2$, respectively. In part (d) the structure factor $H_D(q)$ is compared for three different chain lengths, using $c = 0.5$.

data on the grounds that our chain lengths are too short for the studied concentrations. Thus our conclusion is that our data cannot be taken as evidence for equation (11), simply because there is no extended range of q for which a power law can be observed. On the other hand, we cannot really claim that our data prove that equation (11) is incorrect, however: it is clear that in the simulation the condition $\ell \ll \xi \ll \langle R_g^2 \rangle^{1/2}$, where "$\ll$" means a difference of more than an order of magnitude, is not satisfied, and thus smooth crossovers between the different regimes mask any possible power laws. In the experiment of Jannink *et al.* [6], the condition $\ell \ll \xi$ is not satisfied either, and hence the good agreement with equation (11) reported in reference [6] seems to us somewhat surprising. For the melt case ($c = 2.0$ in our units), on the

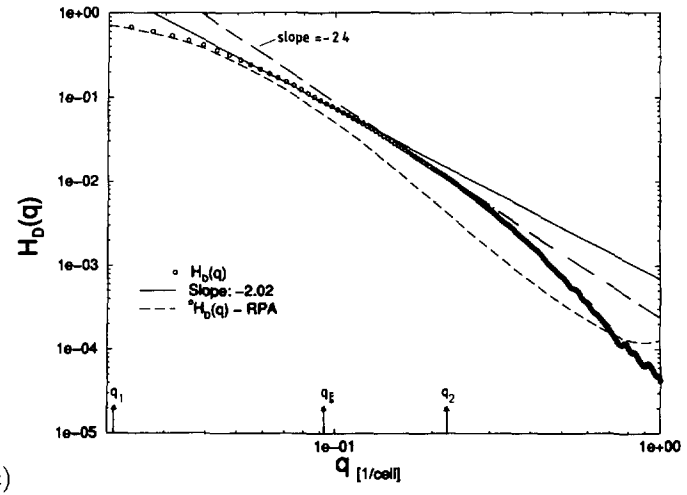

c)

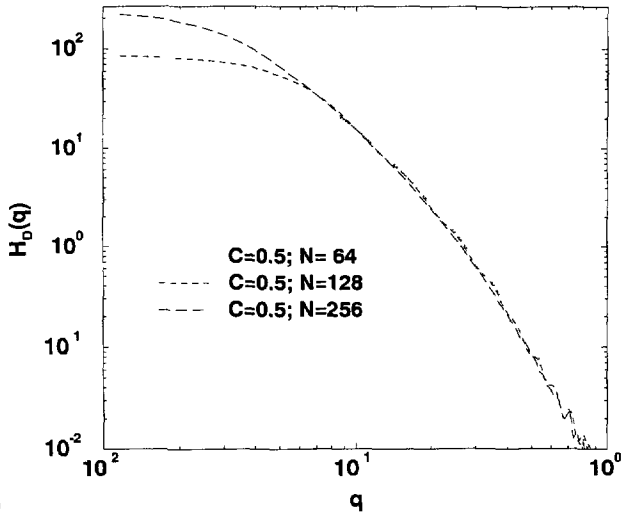

d)

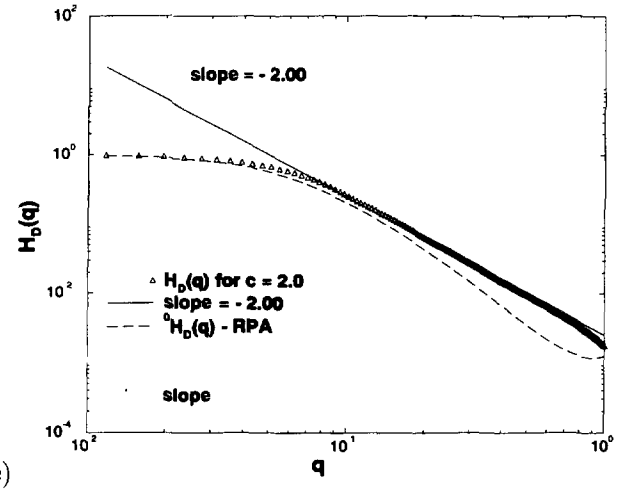

e)

Fig. 6. — *(Continued.)*

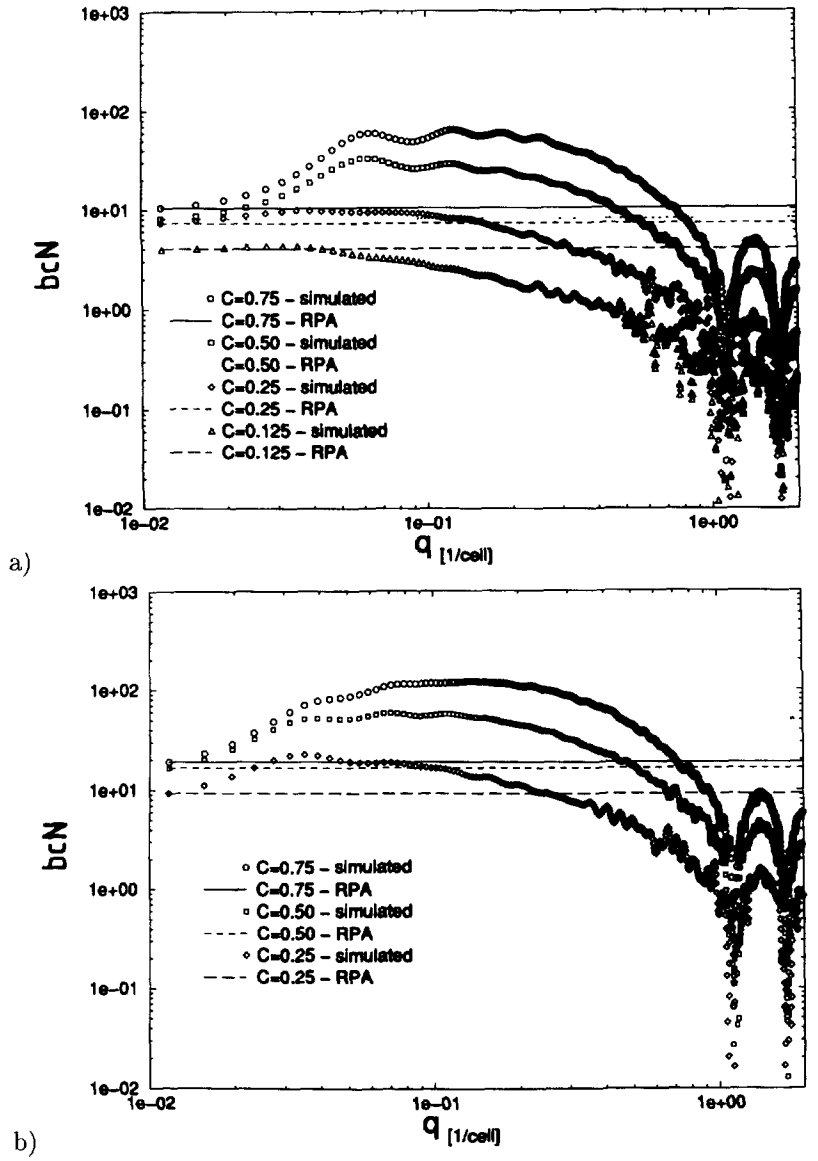

Fig. 7. — log-log plot of the quantity bcN defined empirically by equation (22), for $N = 128$ (a) and $N = 256$ (b). If the RPA were valid, all data should coincide with the corresponding horizontal straight lines shown.

other hand, one finds the expected behavior $H_D(q) \propto h(q) \propto q^{-2}$ over a wide range. Also the RPA is much better now.

To highlight the deviations from RPA, we plot the quantity bcN defined in equation (22) *vs.* q (Fig. 7). It is seen that systematic and pronounced deviations from RPA do indeed occur. While in the dilute case these deviations fall below the straight line for intermediate values of q, the deviations fall above the straight line for larger concentrations. Thus there is a concentration where for a rather large range of q the RPA happens to be rather good

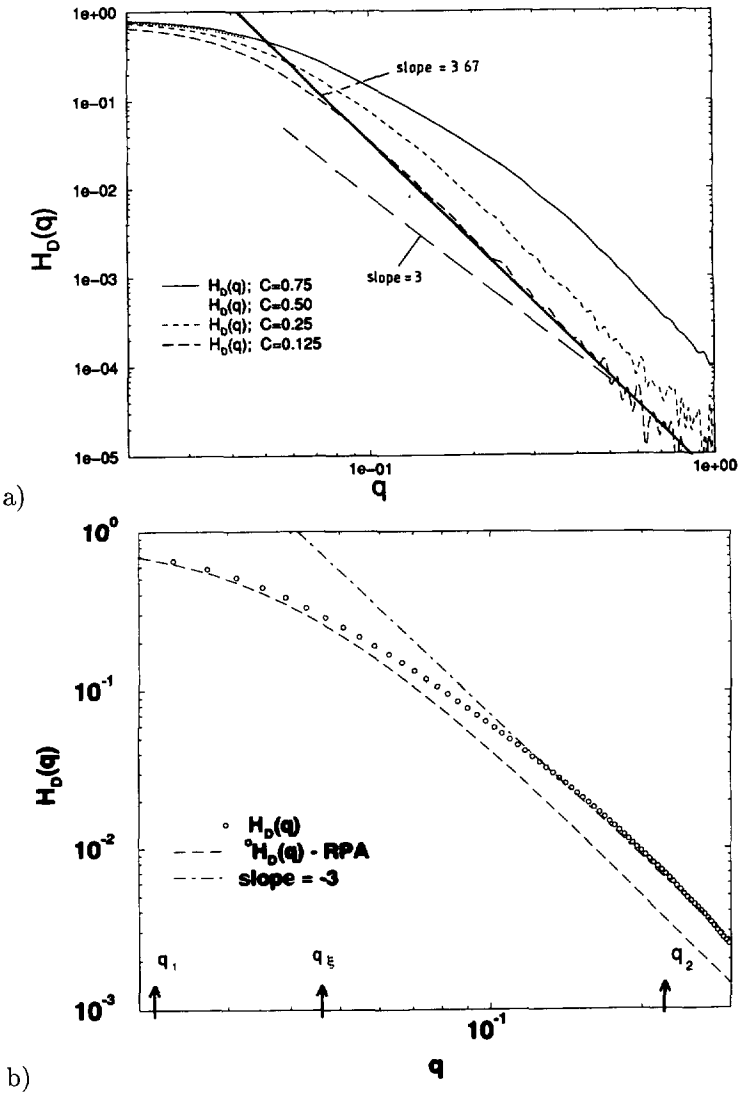

Fig. 8. — a) log-log plot of $H_D(q)$ *vs.* q, comparing for $N = 128$ four concentrations, $c = 0.125$, 0.25, 0.5 and 0.75. b) Expanded part of a $H_D(q)$ *vs.* q plot, for $c = 0.25$ and $N = 256$, showing that a fit to q^{-3} is possible if the q-range is restricted enough.

($c = 0.25$ for $N = 128$, in the crossover regime from dilute to semidilute concentration), but this of course is an accidental cancellation of these opposing tendencies. For $q > q_2$ the data always fall below the RPA prediction.

5. Discussion

While we have obtained clear evidence that the RPA is a very unsatisfactory description of collective scattering from either dilute or semidilute solutions, we have not been able to clearly attribute the cause of these deviations to the corresponding theoretical prediction (Eq. (11)).

We summarize the problem by presenting a comparative plot of $H_D(q)$ for a wide regime of concentrations in Figure 8a: for semidilute concentrations, $H_D(q)$ on the log-log plot is continuously curved, and thus there is clearly no extended q-range where $H_D(q) \propto q^{-3}$ holds. For the more dilute case, $c = 0.125$, there is a rather broad regime where a simple power law seems to hold, but the exponent is wrong. $H_D(q) \propto q^{-3\,67}$ rather than q^{-3}. Possibly, this is due to the competing effect of a correction term with a larger exponent, but this is not clear from the data, in particular since we can no longer measure $H_D(q)$ accurately when it is numerically very small, obviously there are problems with statistical noise in the data for $H_D(q) \ll 10^{-3}$

On the other hand, there is *not* a real discrepancy with the experimental findings of reference [6]: when we look at $H_D(q)$ over a q-range similary restricted as in the experiment for values of q where the RPA just has begun to deviate strongly from the data, we can see a very limited region where $H_D(q) \propto q^{-3}$ seems to be compatible with the data (Fig. 8b). In fact, Figure 8b has a clear similarity with the corresponding Figure 2 of reference [6] (note, however, that the RPA in our case is not a best overall fit to the data, but simply fits only the limit $q \to 0$, and thus discrepancies with the RPA are larger in our case). Although, Figure 8b is so similar to the experiment [6], we do feel that it is no evidence for equation (11), in view of the more extended data shown in Figure 8a. Despite a large effort in computing time, clear conclusions whether equation (11) applies or have not emerged. A possible reason for this failure, of course, is that the conditions $\ell \ll \xi \ll \langle R_g^2 \rangle^{1/2}$ must be stringently satisfied, in order that equation (11) is applicable. On the other hand, the experiment [6] that motivated our study could not satisfy the condition $\ell \ll \xi$ (and hence study the regime $q\xi \gg 1$) either. Clearly, our simulation technique restricts us to study much shorter chains than experimentally. However, one should have expected that in the regime $c \gg c^*$ the chain length is no longer very important, so it was not *a priori* clear that the chain lengths accessible to simulations are too short to clarify this problem. On the other hand, we study a much larger range of q and several concentrations, and thus our conclusions are not just based on a single log-log plot over a rather restrictive q range (Fig. 2 of Ref. [6]) as the experiment. In view of this situation, more extensive work (both experimentally, theoretically and with simulations) seems to us necessary, before one can say that the nature of correlations in polymeric solutions is understood.

Acknowledgments

One of us (K.B.) is very grateful to Prof. G. Jannink for drawing his attention to reference [6] and for suggesting to look into this problem with simulations. This research was partially supported by the Deutsche Forschungsgemeinschaft (DFG), grant N° 436 BUL 113/45 and by the Bulgarian National Science Foundation under grant X-301.

References

[1] Flory P.J. and Bueche A.M., *J. Polym. Sci.* **27** (1958) 219.
[2] des Cloizeaux J., *J. Phys. France* **36** (1975) 281.
[3] Daoud M., Cotton J.P., Farnoux B., Jannink G., Sarma G., Benoit H., Duplessix R., Picot C. and de Gennes P.G., *Macromolecules* **8** (1975) 804.
[4] de Gennes P.G., Scaling Concepts in Polymer Physics, (Cornell University Press, Ithaca, 1979).

[5] des Cloizeaux J. and Jannink G., Polymers in Solution, (Oxford University Press, Oxford, 1990).
[6] Jannink G., Pfeuty P., Lapp A. and Cotton J.P., *Europhys. Lett.* **27** (1994) 47.
[7] Paul W., Binder K., Heermann D.W. and Kremer K., *J. Phys. II France* **1** (1991) 37.
[8] Gerroff I., Milchev A., Binder K. and Paul W., *J. Chem. Phys.* **98** (1993) 6526.
[9] K. Binder, Ed., Monte Carlo and Molecular Dynamics Simulations in Polymer Science (Oxford University Press, New York, Oxford, 1995).
[10] Ullman R., Benoit H. and King J.S., *Macromolecules* **19** (1986) 183.
[11] Le Guillou J.C. and Zinn-Justin J., *Phys. Rev. B* **21** (1980) 3976.
[12] Le Guillou J.C. and Zinn-Justin J., *J. Phys. Lett. France* **46** (1985) L-137.
[13] Le Guillou J.C. and Zinn-Justin J., *J. Phys. France* **50** (1989) 1365.
[14] des Cloizeaux J., Conte R. and Jannink G., *J. Phys. Lett. France* **46** (1985) L-595.
[15] Muthukumar M. and Nickel B.G., *J. Chem. Phys.* **86** (1987) 460.
[16] Li B., Madras N. and Sokal A.D., *J. Statist. Phys.* **80** (1995) 661.
[17] Jannink G., private communication.
[18] Milchev A., Paul W. and Binder K., *J. Chem. Phys.* **99** (1993) 4786.
[19] Milchev A. and Binder K., *Macromol. Theory Simul.* **3** (1994) 915.
[20] Zimm B., *J. Chem. Phys.* **16** (1948) 1093.